A Multi-year Multi-passband CCD Photometric Study of the W UMa Binary EQ Tauri

Kevin B. Alton
UnderOak Observatory, 70 Summit Avenue, Cedar Knolls, NJ 07927

Received June 5, 2009; revised August 7, 2009; accepted September 1, 2009

Abstract A revised ephemeris and updated orbital period for EQ Tau have been determined from newly acquired (2007–2009) CCD-derived photometric data. A Roche-type model based on the Wilson-Devinney code produced simultaneous theoretical fits of light curve data in three passbands by invoking cold spots on the primary component. These new model fits, along with similar light curve data for EQ Tau collected during the previous six seasons (2000–2006), provided a rare opportunity to follow the seasonal appearance of star spots on a W UMa binary system over nine consecutive years. Fixed values for q, $\Omega_{1,2}$, T_1, T_2, and i based upon the mean of eleven separately determined model fits produced for this system are hereafter proposed for future light curve modeling of EQ Tau. With the exception of the 2001 season all other light curves produced since then required a spotted solution to address the flux asymmetry exhibited by this binary system at Max I and Max II. At least one cold spot on the primary appears in seven out of twelve light curves for EQ Tau produced over the last nine years, whereas in six instances two cold spots on the primary star were invoked to improve the model fit. Solutions using a hot spot were less common and involved positioning a single spot on the primary constituent during the 2001–2002, 2002–2003, and 2005–2006 seasons.

1. Introduction

The variability of EQ Tauri was discovered by Tsesevich (1954) but was not rigorously characterized until the first modern orbital period was reported by Whitney (1972). Thereafter largely neglected for over two decades, Benbow and Mutel (1995) produced the first CCD-derived (R) light curve found in the literature. More recently, photoelectric (*UBV*) studies by Pribulla *et al.* (2001) and Vaňko *et al.* (2004) have been published along with more robust multi-color CCD investigations by Yang and Liu (2002), Zola *et al.* (2005), Hrivnak *et al.* (2006), Csizmadia *et al.* (2006b), and Yuan and Qian (2007). A period study of EQ Tau was conducted by Qian and Ma (2001), who comprehensively analyzed times of minimum light over a twenty-three year period from 1973 to 1996.

Similar to the Sun, EQ Tauri is spectral type G2 but due to mutual eclipses its visual magnitude changes from 10.3 to 11 every 0.341349 day. Since the most massive (1.22 $M_\odot$) and hotter primary star is occulted (annular eclipse) by

the less massive (0.539 $M_{\odot}$) but cooler secondary constituent during primary minimum, EQ Tau belongs to the A-type subclass of W UMa binaries (Binnendijk 1984). With an orbital inclination approaching 86°, our view of this system is nearly edge on. This relatively bright variable is easily within the light grasp of a modest aperture telescope coupled with a consumer-grade CCD camera. In the neighborhood, but not part of the Pleiades (~2° southeast), EQ Tau is well positioned for mid-latitude observers in the Northern Hemisphere during the fall and winter months.

Being one of the more frequently studied W UMa binary systems, existing Wilson-Devinney modeling data which cover 2000–2006 combined with new data collected between 2006 and 2009 provides a unique opportunity to refine our understanding of EQ Tau. Significant changes to physical or geometric elements such as effective stellar temperature (T_1 and T_2), Roche potential ($\Omega_{1,2}$), inclination angle (i), and mass ratio ($q = m_2/m_1$) generally occur over millennia. There is a reasonable expectation that values for each of these parameters should have remained fairly constant over the past decade, yet an unrealistically wide range in values is found in the literature (Table 1). Therefore a strategy was developed to fix values for i, $\Omega_{1,2}$, T_1, T_2, and q, so that the latest (2006–2009) epochal variations in light curve morphology could potentially be more accurately modeled, in this case by the addition of putative spot(s).

2. Observations and data reduction

2.1. Photometry

Images of EQ Tau were matched against the standard star fields provided in MPO CANOPUS (version 9.5.0.3; Minor Planet Observer 2003) as described previously for SW Lac (Alton and Terrell 2006). CCD photometric imaging began on December 10, 2006, with the intent of generating light curves over three consecutive years which could be used to: 1) refine the orbital period for EQ Tau; 2) calculate an updated ephemeris; and 3) potentially track the course of starspots known to appear in this binary system. Equipment included a 0.2-m Celestron Nexstar 8 GPS (f/6.3) with an SBIG ST-402ME CCD camera mounted at the Cassegrain focus. The field of view (FOV) produced by this configuration was 12.3 × 18.5 arcmin (1.45 arcsec/pixel). Multi-passband imaging was automatically performed with SBIG photometric B, V, and I_c filters (consistent with Bessell standard definition) mounted onto a multi-position wheel. Each exposure was captured (unbinned) over a 20- to 45-second period with thermoelectric cooling regulated to maintain the CCD chip at –5°C. Typical sessions lasted from two to four hours with I_c, V, and B images taken in immediate succession. Computer clock time was updated via the Internet Time Server immediately prior to each session. Image acquisition (raw lights, darks, and flats) was performed using SBIG CCDSOFT 5 (version 5.00.174) while calibration and registration was accomplished with AIP4WIN (version 2.1.10;

Berry and Burnell 2000). Further photometric reduction (circular aperture) with MPO CANOPUS was achieved using two non-varying comparison stars (TYC1260-00575-1, $V=10.4$, $B–V=1.1$; and TYC1260-00893-1, $V=9.49$, $B–V=0.74$) to ultimately generate light curves for calculating ephemerides and orbital period. Instrumental readings were not reduced to standard magnitudes.

2.2. Light curve analyses

Preliminary light curve fits and final geometric renderings were produced by BINARY MAKER (version 3.0; Bradstreet and Steelman 2002). Light curve modeling was performed using PHOEBE (Prša and Zwitter 2005) and WDWINT (Nelson 2005b), both of which employ the W-D code (Wilson and Devinney 1971; Wilson 1979). PHOEBE is an elegant implementation of the W-D code which provides a very convenient as well as enhanced user interface. Each model fit incorporated individual observations and not binned to normal points. SIGMA was assigned according to the standard deviation measured from the average difference in instrumental magnitude (C_{avg}) for each comparison star. For the *B*, *V*, and I_c passbands, variability was typically ±0.03, ±0.01, and ±0.01, respectively.

3. Results and discussion

3.1. Ensemble photometry

A representative exposure (20 seconds) taken in *V*-band showing EQ Tau along with two comparison stars from the Tycho 2 catalog is reproduced in Figure 1. Prior to accepting processed results from each session, comparison stars were tested for variability over the observation period. A typical example is shown for a dataset in *V* acquired on February 18, 2008 (Figure 2). Collectively, C_{avg} in I_c, *V*, or *B* passband did not exhibit a pattern or trend that would otherwise suggest variability beyond experimental error.

3.2. Folded light curve and ephemeris

A total of 2,123 individual photometric readings in *B*, 2,134 in *V*, and 2,144 in I_c were combined within each passband to produce three seasonal light curves (2007, 2008, and 2009) that spanned 778 days of data collection. These observations included forty-two new times of minima (ToM) which were captured between December 10, 2006, and January 4, 2009 (Table 2). CANOPUS provided a period solution for the folded datasets using Fourier analysis. The time of minimum for the first primary epoch was estimated by CANOPUS using the Hertzsprung method as detailed by Henden and Kaitchuck (1990). The linear ephemeris equation (1) for the Heliocentric Primary Minimum (HPM) was initially determined to be:

$$HPM = 2454520.5788 + 0.341349\,(2)\,E \qquad (1)$$

and in excellent accordance with previously published orbital periods (d) for EQ Tau. A periodogram (Figure 3), produced using PERANSO (version 2.31; Vanmunster 2005) by applying periodic orthogonals (Schwarzenberg-Czerny 1996) to fit observations and analysis of variance (ANOVA) to evaluate fit quality, reaffirmed the period determination. ToM values (Table 2) were estimated by the program MINIMA (version 24d; Nelson 2005a) using the simple mean from a suite of six different methods including: parabolic fit, tracing paper, bisecting chords, Kwee and van Woerden (1956), Fourier fit, and sliding integrations (Ghedini 1981). These new minima along with values from Pribulla and Vanko (2002), Yang and Liu (2002), Yuan and Qian (2007), Hrivnak *et al.* (2006), Alton (2006), and additional observations published (*IBVS, AAVSO, VSOLJ,* as given in the reference list) between 2001 and 2008 or readings otherwise posted on the B.R.N.O. Project website

(http://var.astro.cz/ocgate/ocgate.php?star=EQ+Tau&lang=en)

were used to calculate residual values based upon the GCVS reference epoch (Kholopov *et al.* 1985) defined by the ephemeris (2):

$$\mathrm{HPM} = 2440213.3250 + 0.341348\,\mathrm{E} \quad (2)$$

Two separate regression analyses were performed due to the curvilinear nature of the O–C residuals observed for at least a decade. A revised equation (3) based upon a linear least squares fit (Figure 4) of near term (O–C)1 data from October 2, 2005, to January 4, 2009 was calculated from:

$$\mathrm{O–C} = a + bE \quad (3)$$

where:

$a = -4.0414 \times 10^{-2} \pm 2.0806 \times 10^{-3}$
$b = 3.4355 \times 10^{-7} \pm 5.0322 \times 10^{-8}$

$$\mathrm{HPM} = 2440213.2846\,(21) + 0.341349\,(1)\,\mathrm{E} \quad (4)$$

Expanding the analysis to include a notably rich ($n > 150$) set of photometrically-derived ToM data from the past nine years revealed a parabolic relationship (Figure 5) between residuals $(O–C)_1$ and HJD that can be fit by the quadratic expression (5):

$$\mathrm{O–C} = a + bE + cE^2 \quad (5)$$

where:

$a = 9.5316 \times 10^{-2} \pm 1.5271 \times 10^{-2}$
$b = -6.3369 \times 10^{-6} \pm 7.9365 \times 10^{-7}$
$c = 8.2080 \times 10^{-11} \pm 1.0265 \times 10^{-11}$

which leads to the following ephemeris (6):

$$\mathrm{HPM} = 2440213.4207\,(153) + 0.341321\,(1)\,\mathrm{E} + 8.21(103) \times 10^{-11}\,\mathrm{E}^2 \quad (6)$$

From the fall of 2000 and on consecutive years through 2009, EQ Tau has

apparently experienced a very slow orbital period increase as defined by equation (7):

$$dP/dt = 2 \times (8.21 \times 10^{-11})(1/0.341321)(86400)(365.25) \quad (7)$$
$$= 0.01518 \text{ sec/yr}$$

Interestingly, Qian and Ma (2001) reported a negative parabolic fit in previous years (1973–1997), which corresponded to a secular decrease in the orbital period (dP/dt = –0.016 sec/yr). Unfortunately there is a paucity of published observations for EQ Tau between 1997 and 2000 so that the transition between positive and negative orbital period rate changes was not captured. Nonetheless, this fluctuation in periodicity is not uncommon behavior for W UMa type variables, as discussed by Dryomova and Svechnikov (2006). Therein it is suggested that according to thermal relaxation oscillation (TRO) theory, thermal oscillations begin to temporarily disrupt the contact phase when the mass ratio (q) approaches a value of 0.45. The cycle of contact breakup and restoration due to the inability to simultaneously achieve thermal and dynamic equilibrium could potentially explain the succession of increasing and decreasing orbital periods often observed with W UMa binaries like EQ Tau.

Folded light curves in B, V, and I_c, show that both minima are separated by ~0.5 phase and are consistent with a circular orbit (Figure 6). As has been reported by a number of investigators including Yang and Liu (2002) and Pribulla and Vaňko (2002), the so-called O'Connell effect was also observed in all new light curves described herein. This asymmetry, common to many light curves from overcontact binaries, exhibited its greatest effect in the I_c band, where in all cases Max I > Max II. One plausible explanation for this intrinsic variability involves the presence of starspot(s) on one or more binary components and is examined further in section 3.3.1.

3.3. Light curve synthesis

The Roche model derived from the seminal Wilson and Devinney (1971) paper has been widely applied to produce simulated light curve solutions which closely fit changes in flux arising from eclipsing star systems. Collectively, synchronous rotation, no third light (l3 = 0), and circular orbits (e = 0) were defined as constants within PHOEBE using the "overcontact binary not in thermal contact" model. Bolometric albedo ($A_{1,2} = 0.5$) and gravity darkening coefficients ($g_{1,2} = 0.32$) for cooler stars with convective envelopes were according to Ruciński (1969) and Lucy (1967), respectively. Logarithmic limb darkening coefficients (x_1, x_2, y_1, y_2) for both stars were interpolated within PHOEBE according to Van Hamme (1993) after any change in T_{eff}. The mean effective temperature of star 1 (the star eclipsed at primary minimum) was set equal to 5800K based on its spectral type (G2). Radial velocity measurements previously performed on EQ Tau (Ruciński *et al.* 2001) provided a spectroscopically determined value for the mass ratio ($q = 0.442$) which helped constrain the many possible solutions.

Once an approximate fit was obtained, differential corrections (DC) were applied simultaneously to photometric data in all filters. Standard errors for the present study (Table 1) are those calculated by WDWINT (Nelson 2005b).

3.3.1. Unspotted and spotted models

Since immediate visual feedback from each synthetic light curve iteration is possible in PHOEBE, this application proved to be particularly adept at rapidly reaching a convergent solution. As a starting point for an unspotted solution, the *V*-band values for q, $\Omega_{1,2}$, T_1, T_2, and i reported by Alton (2006) were used. For each epoch, $A_{1,2}$, $g_{1,2}$, $x_{1,2}$, and T_1 were fixed, whereas $\Omega_{1,2}$, T_2, q, and i were iteratively adjusted using DC to achieve a minimum simultaneous residual fit of *B*, *V*, and I_c photometric observations. As was the case with all new light curves described herein, the unspotted W-D model error $[\Sigma(O–C)^2]$, where O–C is the residual between the observed and synthetic light curve, was unacceptable due to the poor coverage of the light curve especially during Max I and Min II. This is visually obvious in a representative example taken from photometric data (I_c) collected in early 2009 (Figure 7).

The excess flux during Max I suggested starspot solution(s) for the 2007–2009 epochs. Yang and Liu (2002) were the first to reproduce the asymmetrical shape of EQ Tau light curves by employing the geometrical and physical elements (A_S, Θ, ψ, and r_S) of hot and dark starspots on each stellar component. The asymmetry observed at Max I for EQ Tau may arise from a number of possibilities, including: 1) cold starspot(s) on either component facing the observer to decrease the depth of Max II, or 2) hot starspot(s) on either star responsible for an increase in flux during Max I. It is clear from the recent literature, which covers five consecutive years (2000–2006) of light curves for EQ Tau, that both cold and hot starspots have been successfully used to minimize the residual fit of the Roche model (Table 1). Since seasonal variations in light curves from W UMa binary systems are well documented, data from each new epoch (2007, 2008, and 2009) were modeled independently but using the same seed values (*V*-band) for q, $\Omega_{1,2}$, T_1, T_2, and i initially reported by Alton (2006). Newly fit values for q, T_2, and i were averaged with literature values reported between 2000 and 2004 (Table 1) and thereafter, along with T_1 (5800K), entered afresh as fixed values. In all three cases (2007, 2008, and 2009), DC iterations of A_S, Θ, ψ, and r_S yielded a best fit which supported placement of two cold starspots on the primary constituent (Figure 8). An additional cold spot was positioned on the secondary star to improve the model fit to the 2008 light curves. Synthetic light curves superimposed upon *B*, *V*, and I_c passband data are illustrated in Figure 9 (2007), Figure 10 (2008), and Figure 11 (2009). Using PHOEBE, an improved fit of the 2005–2006 light curves (*V* and *R*) previously produced by this author (Alton 2006) was obtained by adding a cold spot to the primary star. Interestingly, this would appear to be the only epoch over the past nine years in which Max II > Max I. However,

as previously noted (Alton 2006), the large gap in *R*-band data around Max II (Figure 12) does leave some doubt about the robustness of the model fit.

With the exception of the 2001 light curves generated by Vaňko *et al.* (2004), all other light curves produced since 2000 required a spotted solution to address the flux asymmetry exhibited by this binary system at Max I and Max II. Even in this case the authors suggested the possibility of cool spot(s) but refrained from introducing any spot during modeling due to the poor quality and photometric coverage at Max I. At least one cold spot on the primary has figured prominently in the simulated W-D solution in seven out of twelve light curves for EQ Tau produced since 2000. In six instances—2000, 2004 (two different solutions), 2007, 2008, and 2009—two cold spots on the primary star were invoked to improve the model fit. Solutions using a hot spot were less common and involved positioning a single spot on the primary constituent during the 2001–2002, 2002–2003, and 2005–2006 seasons.

4. Conclusions

Filtered (*B*, *V*, and I_c) CCD-based photometric readings have lead to forty-two new times of minima and the construction of light curves between 2007 and 2009 which were used to revise the orbital period for EQ Tau and calculate an updated ephemeris. A positive parabolic relationship between O–C residuals and cycle number continues to suggest a secular rate increase in dP/dt which started over a decade ago. Fixed values for q, $\Omega_{1,2}$, T_1, T_2, and i were calculated from the mean of eleven independently determined model fits produced for this system over nine consecutive years. A Roche-type model invoking cold spots primarily on the more massive constituent produced simultaneous theoretical fits of light curve data in three passbands between 2006 and 2009 that largely account for the asymmetrical flux intensity at maximum light. This result is not unexpected since cold spots on the primary star are featured in the simulated models for seven of twelve light curves produced since 2000.

5. Acknowledgements

The many constructive comments suggested by the referee are greatly appreciated. Special thanks are due to the NASA Astrophysics Data System hosted by the Computation Facility at the Harvard-Smithsonian Center for Astrophysics without which this research effort would not be possible. This investigation has also made use of the SIMBAD database, operated at CDS, Strasbourg, France, and the B.R.N.O. Project database generously maintained by the Czech Astronomical Society.

References

Agerer, F., and Hübscher, J. 2002, *Inf. Bull. Var. Stars*, No. 5296.

Agerer, F., and Hübscher, J. 2003, *Inf. Bull. Var. Stars*, No. 5484.

Alton, K. 2006, *Open European J. Var. Stars*, **39**, 1.

Alton, K. B., and Terrell, D. 2006, *J. Amer. Assoc. Var. Star Obs.*, **34**, 188.

Baldwin, M. E., and Samolyk, G. 2002, *Observed Minima Timings of Eclipsing Binaries No. 7*, AAVSO, Cambridge, MA.

Baldwin, M. E., and Samolyk, G. 2005, *Observed Minima Timings of Eclipsing Binaries No. 10*, AAVSO, Cambridge, MA.

Baldwin, M. E., and Samolyk, G. 2007, *Observed Minima Timings of Eclipsing Binaries No. 12*, AAVSO, Cambridge, MA.

Benbow, W. R., and Mutel, R. L. 1995, *Inf. Bull. Var. Stars*, No. 4187.

Berry, R., and Burnell, J. 2000, "Astronomical Image Processing Software," version 2.1.10, provided with *The Handbook of Astronomical Image Processing*, WIllmann-Bell, Richmond, VA.

Binnendijk, L. 1984, *Publ. Astron. Soc. Pacific*, **96**, 646.

Bíró, I. B., *et al.* 2007, *Inf. Bull. Var. Stars*, No. 5753.

Bradstreet, D. H., and Steelman, D. P. 2002, *Bull. Amer. Astron. Soc.*, **34**, 1224.

Borkovits, T., Bíró, I. B., Csizmadia, S., Patkós, L., Hegedüs, T., Pál, A. Kóspál, Á., and Klagyivik, P. 2004, *Inf. Bull. Var. Stars*, No. 5579.

Cook, J. M., Divoky, M., Hofstrand, A., Lamb, J., and Quarderer, N. 2005, *Inf. Bull. Var. Stars*, No. 5636.

Csizmadia, Sz., Klagyivik, P., Borkovits, T., Patkós, L., Kelemen, J., Marschalkó, G., and Marton, G. 2006a, *Inf. Bull. Var. Stars*, No. 5736.

Csizmadia, Sz., Kővári, Z., and Klagyivik, P. 2006b, *Astrophys. Space Sci.*, **304**, 355.

Csizmadia, Sz., Zhou, A. Y., Könyves, V., Varga, Z., and Sándor, Zs. 2002, *Inf. Bull. Var. Stars*, No. 5230.

Diethelm, R. 2003, *Inf. Bull. Var. Stars*, No. 5438.

Dogru, S. S., Dogru, D., and Dönmez, A. 2007, *Inf. Bull. Var. Stars*, No. 5795.

Dryomova, G. N., and Svechnikov, M. A. 2006, *Astrophys.*, **49**, 358.

Ghedini, S. 1981, *Mem. Soc. Astron. Italiana*, **52**, 633.

Henden, A. A., and Kaitchuck, R. H. 1990, *Astronomical Photometry: A Text and Handbook for the Advanced Amateur and Professional Astronomer*, Willmann-Bell, Richmond.

Hrivnak, B. J., Lu, W., Eaton, J., and Kenning, D. 2006, *Astron. J.*, **132**, 960.

Hübscher, J. 2005, *Inf. Bull. Var. Stars*, No. 5643.

Hübscher, J., Paschke, A., and Walter, F. 2005, *Inf. Bull. Var. Stars*, No. 5657.

Hübscher, J., Paschke, A., and Walter, F. 2006, *Inf. Bull. Var. Stars*, No. 5731.

Hübscher, J., and Walter, F. 2007, *Inf. Bull. Var. Stars*, No. 5761.

Kholopov, P. N., *et al.* 1985, *General Catalogue of Variable Stars*, 4th ed., Moscow.

Krajci, T. 2005, *Inf. Bull. Var. Stars*, No. 5592.

Kwee, K. K., and van Woerden, H. 1956, *Bull. Astron. Inst. Netherlands*, **12**, 327.
Lucy, L. B. 1967, *Z. Astrophys.*, **65**, 89.
Minor Planet Observer 2003, MPO Software Suite, BDW Publishing, Colorado Springs (http://www.minorplanetobserver.com).
Müyesseroglu, Z., Törün, E., Özdemir, T., Gürol, B., Özavci, I., Tunç, T., and Kaya, F. 2003, *Inf. Bull. Var. Stars*, No. 5463.
Nagai, K. 2004, *VSOLJ Variable Star Bulletin*, No. 42.
Nagai, K. 2009, *VSOLJ Variable Star Bulletin*, No. 48.
Nelson, R. H. 2001, *Inf. Bull. Var. Stars*, No. 5040.
Nelson, R. H. 2003, *Inf. Bull. Var. Stars*, No. 5371.
Nelson, R. H. 2004, *Inf. Bull. Var. Stars*, No. 5493.
Nelson, R. H. 2005a, MINIMA astronomy software, URL:http://members.shaw.ca/bob.nelson/software1.htm.
Nelson, R. H. 2005b, WDWINT (version 5.4e) astronomy software, URL: http://members.shaw.ca/bob.nelson/software1.htm.
Nelson, R. H. 2008, *Inf. Bull. Var. Stars*, No. 5820.
Parimucha, Š., *et al.* 2007, *Inf. Bull. Var. Stars*, No. 5777.
Pribulla, T., and Vaňko, M. 2002, *Contrib. Astron. Obs. Skalnaté Pleso*, **32**, 79.
Pribulla, T., Vaňko, M., Parimucha, Š., and Chochol, D. 2001, *Inf. Bull. Var. Stars*, No. 5056.
Pribulla, T., *et al.* 2005, *Inf. Bull. Var. Stars*, No. 5668.
Prša, A., and Zwitter, T. 2005, *Astrophys. J.*, **628**, 426.
Qian, S., and Ma, Y. 2001, *Pub. Astron. Soc. Pacific*, **113**, 754.
Ruciński, S. M. 1969, *Acta Astron.*, **19**, 245.
Rucin´ski, S. M., Lu, W., Mochnacki, S. W., Ogloza, W., and Stachowski, G. 2001, *Astron. J.*, **122**, 1974.
Šarounová, L., and Wolf, M. 2005, *Inf. Bull. Var. Stars*, No. 5594.
Schwarzenberg-Czerny, A. 1996, *Astrophys. J., Lett. Ed.*, **460**, L107.
Tsesevich, V. P. 1954, *Izv. Astron. Obs. Odessa*, **4**, No. 3.
Van Hamme, W. 1993, *Astron. J.*, **106**, 2096.
Vaňko, M., Parimucha, Š., Pribulla, T., and Chochol, D. 2004, *Baltic Astron.*, **13**, 151.
Vanmunster, T. 2005, PERANSO period analysis software, www.peranso.com
Whitney, B. S. 1972, *Inf. Bull. Var. Stars*, No. 633.
Wilson, R. E. 1979, *Astrophys. J.*, **234**, 1054.
Wilson, R. E., and Devinney, E. J. 1971, *Astrophys. J.*, **166**, 605.
Yang, Y., and Liu, Q. 2002, *Astron. J.*, **124**, 3358.
Yuan, J., and Qian, S. 2007, *Mon. Not. Roy. Astron. Soc.*, **381**, 602.
Zola, S., *et al.* 2005, *Acta Astron.*, **55**, 389.

Table 1. Comparison of light curve parameters and geometric elements determined for EQ Tau between 2000 and 2009.

Parameter	*Yuan and Qian (2007) 2000*	*Pribulla and Vaňko (2002) 2001*	*Yang and Liu (2002) 2001 D2*	*Yang and Liu (2002) 2001 H1*	*Hrivnak et al. (2006) 2001–2002*	*Hrivnak et al. (2006) 2002–2003*
T_1 (K)	5800	5860	5800	5800	5800	5800
T_2 (K)	5754 (5)	5851 (8)	5735 (4)	5722 (5)	5721 (7)	5721 (7)
q (m_2/m_1)	0.442 (3)	0.442 (7)	0.4457 (11)	0.4347 (15)	0.445 (6)	0.445 (6)
$\Omega_{1,2}$	2.7316 (27)	2.7303 (29)	2.7192 (17)	2.7161 (20)	2.7250 (20)	2.7250 (20)
i°	85.21 (38)	86.59 (69)	84.32 (45)	83.67 (13)	84.7 (2)	84.7 (2)
f (% overcontact)	11.57 (99)	12.0 (1.3)	18.8	12.1	16 (1)	16 (1)
$A_{S1a} = T_{S1}/T_2$	0.64 (6)		0.80 (3)	1.10 (4)	1.10	1.10
Θ_{S1a} (spot colatitude)	14.1° (2.4)		95.8° (6)	103.2° (9)	90°	90°
ψ_{S1a} (spot longitude)	96.8° (2.3)		261.8° (6)	260.9° (8)	257.70 (63)	269.20° (32)
r_{S1a} (angular radius)	30.5° (3.5)		18.6° (1)	14.2° (2)	11.1 (10)	10.8° (4)
$A_{S1b} = T_{S2}/T_2$	0.60 (6)					
Θ_{S1b} (spot colatitude)	165.8° (6.5)					
ψ_{S1b} (spot longitude)	252° (3.2)					
r_{S1b} (angular radius)	38.3° (2.8)					

(Table 1 continued on following page)

Table 1. Comparison of light curve parameters and geometric elements determined for EQ Tau between 2000 and 2009, continued.

Parameter	*Csizmadia et al. (2006b) 2004*	*Yuan and Qian (2007) 2004*	*Alton (2006) 2005–2006*	*Present Study 2006–2007*	*Present Study 2007–2008*	*Present Study 2008–2009*
T_1 (K)	NR	5800	5800	5800	5800	5800
T_2 (K)	NR	5754 (5)	5753 (38)	5753 (38)	5753 (38)	5753 (38)
q (m_2/m_1)	NR	0.442 (3)	0.4406 (56)	0.4406 (56)	0.4406 (56)	0.4406 (56)
$\Omega_{1,2}$	NR	2.7316 (27)	2.7226 (29)	2.7226 (29)	2.7226 (29)	2.7226 (29)
i°	NR	85.21 (38)	85.6 (13)	85.6 (13)	85.6 (13)	85.6 (13)
f (% overcontact)	NR	11.57 (99)	13.96	13.96	13.96	13.96
$A_{S1a} = T_{S1}/T_2$	0.72	0.94 (3)	1.23 (1)	0.878 (8)	0.85 (1)	0.767 (7)
Θ_{S1a} (spot colatitude)	0	34.6° (4.4)	94.2° (16)	112° (3)	94° (2)	86.3° (23)
ψ_{S1a} (spot longitude)	270	96.4° (9.9)	1.23° (38)	130° (3)	175.7° (11)	63.0° (10)
r_{S1a} (angular radius)	15	48.6° (7.8)	15.1° (2)	10.74° (21)	11.4° (6)	13.26° (9)
$A_{S1b} = T_{S2}/T_2$	0.95	0.93 (0.11)	0.818 (8)	0.663 (96)	0.761 (44)	0.585 (2)
Θ_{S1b} (spot colatitude)	0	135.8° (31.5)	103.7° (39)	105.3° (19)	89.4° (98)	29.4° (21)
ψ_{S1b} (spot longitude)	180	288.8° (6.4)	281.5° (30)	186.7° (25)	56° (1)	170.6° (12)
r_{S1b} (angular radius)	10	21.3° (9.5)	13.4° (2)	7.1° (4)	15.5° (1)	17.6° (6)
$A_{S2a} = T_{S1}/T_2$					0.685 (40)	
Θ_{S2a} (spot colatitude)					118° (7)	
ψ_{S2a} (spot longitude)					127.7° (38)	
r_{S2a} (angular radius)					13.9° (4)	

Note: $A_{1,2} = 0.5$; $g_{1,2} = 0.32$; NR = not reported. Values in parenthesis represent the standard error in the rightmost digit(s).

Table 2. Journal of new light curve minima captured from EQ Tauri between December 10, 2006, and January 4, 2009.

Observed Time of Minima (HJD-2400000.0)	*UT Date*	*Passband*	*No. of Observations*	*Type of Minima*
54079.5565± 0.0001	10 Dec 2006	*V*	132[a]	I
54079.5563± 0.0002	10 Dec 2006	*B*	135	I
54079.5566± 0.0003	10 Dec 2006	I_c	133	I
54089.6267± 0.0001	20 Dec 2006	*V*	154	II
54089.6269± 0.0002	20 Dec 2006	*B*	153	II
54089.6262± 0.0001	20 Dec 2006	I_c	151	II
54103.6221± 0.0001	3 Jan 2007	I_c	154	II
54103.6220± 0.0001	3 Jan 2007	*V*	152	II
54103.6221± 0.0002	3 Jan 2007	*B*	156	II
54111.6437± 0.0001	11 Jan 2007	I_c	171	I
54111.6437± 0.0001	11 Jan 2007	*V*	164	I
54111.6424± 0.0042	11 Jan 2007	*B*	169	I
54491.5644± 0.0002	26 Jan 2008	*B*	111[b]	I
54491.5646± 0.0001	26 Jan 2008	I_c	112	I
54491.5645± 0.0001	26 Jan 2008	*V*	112	I
54499.5844± 0.0002	3 Feb 2008	*B*	99	II
54499.5860± 0.0001	3 Feb 2008	I_c	100	II
54499.5861± 0.0001	3 Feb 2008	*V*	99	II
54508.6313± 0.0001	12 Feb 2008	*B*	129	I
54508.6319± 0.0001	12 Feb 2008	I_c	131	I
54508.6313± 0.0001	12 Feb 2008	*V*	133	I
54513.5823± 0.0003	17 Feb 2008	*B*	125	II
54513.5819± 0.0001	17 Feb 2008	I_c	127	II
54513.5824± 0.0002	17 Feb 2008	*V*	125	II
54520.5791± 0.0002	24 Feb 2008	*B*	74	I
54520.5792± 0.0001	24 Feb 2008	I_c	72	I
54520.5791± 0.0001	24 Feb 2008	*V*	77	I
54798.6080± 0.0002	28 Nov 2008	*B*	74[c]	II
54798.6079± 0.0001	28 Nov 2008	I_c	75	II
54798.6077± 0.0001	28 Nov 2008	*V*	74	II
54813.6276± 0.0002	13 Dec 2008	*B*	72	II
54813.6273± 0.0001	13 Dec 2008	I_c	73	II
54813.6277± 0.0002	13 Dec 2008	*V*	73	II
54823.6968± 0.0001	23 Dec 2008	*B*	78	I
54823.6967± 0.0001	23 Dec 2008	I_c	80	I
54823.6964± 0.0001	23 Dec 2008	*V*	80	I

(Table 2 continued on following page)

Table 2. Journal of new light curve minima captured from EQ Tauri between December 10, 2006 and January 4, 2009, continued.

Observed Time of Minima (HJD-2400000.0)	*UT Date*	*Passband*	*No. of Observations*	*Type of Minima*
54830.5234± 0.0001	30 Dec 2008	*B*	58	I
54830.5238± 0.0002	30 Dec 2008	I_c	58	I
54830.5236± 0.0001	30 Dec 2008	*V*	57	I
54835.6440± 0.0002	4 Jan 2009	*B*	111	I
54835.6441± 0.0002	4 Jan 2009	I_c	112	I
54835.6439± 0.0001	4 Jan 2009	*V*	111	I

a: 2007 folded light curves (10 Dec 06—11 Jan 07).
b: 2008 folded light curves (26 Jan 08—10 Mar 08).
c: 2009 folded light curves (28 Nov 08—25 Jan 09).

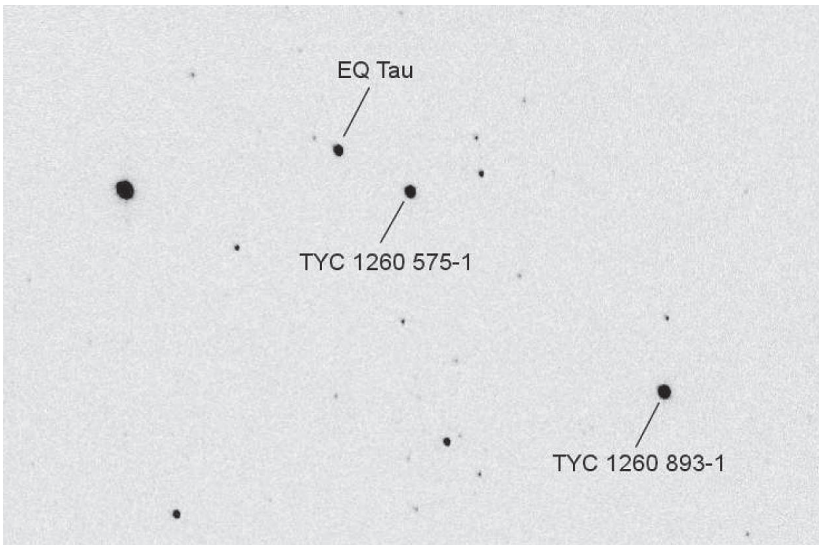

Figure 1. Exposure (20 seconds) in *V*-band taken on December 8, 2006, showing EQ Tau and two comparison stars from the Tycho 2 catalog.

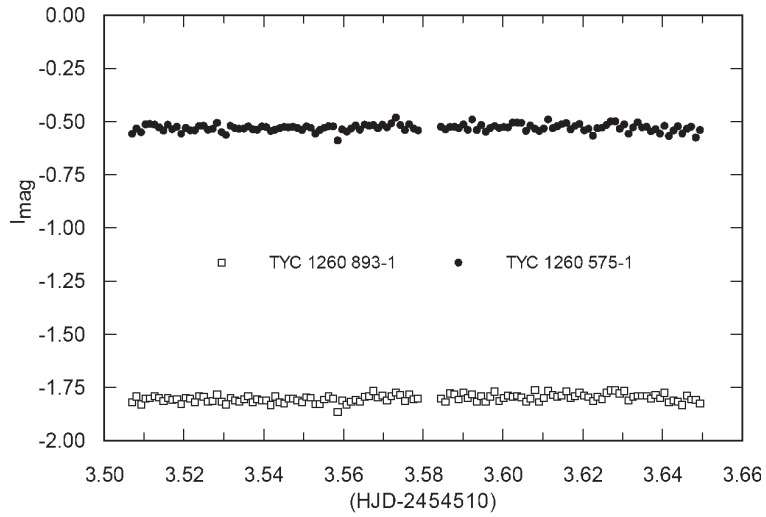

Figure 2. *V*-band instrumental magnitude (Imag) vs time (HJD) for the average magnitude (Cavg) from two comparison stars. Discontinuities in data arise from rejected readings due to the sporadic appearance of clouds.

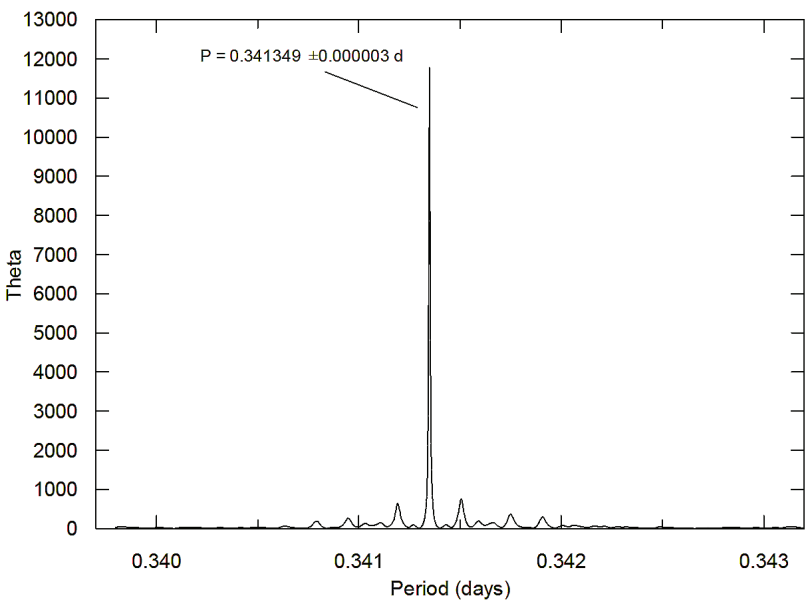

Figure 3. Periodogram for EQ Tau using the Schwarzenberg-Czerny (1996) method to search for periodicity in unevenly sampled observations.

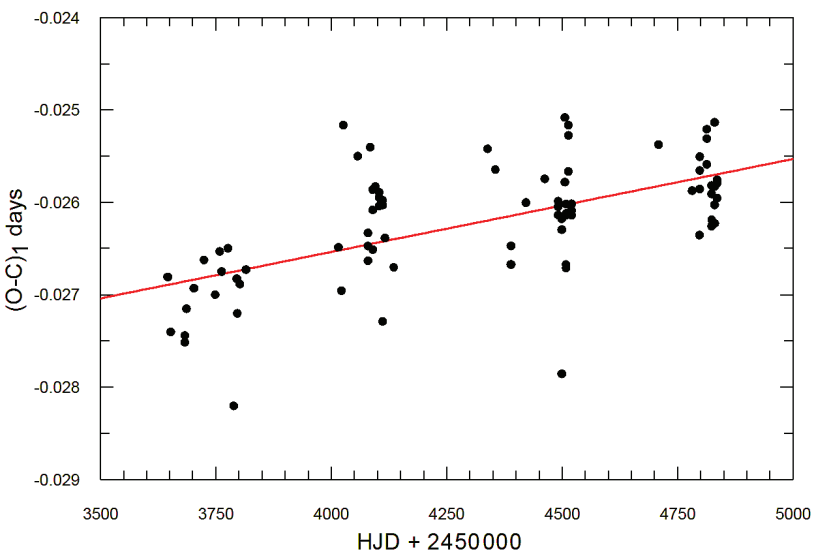

Figure 4. Linear least squares fit of residuals (O–C)1 vs HJD for EQ Tau observed between October 2, 2005, and January 4, 2009.

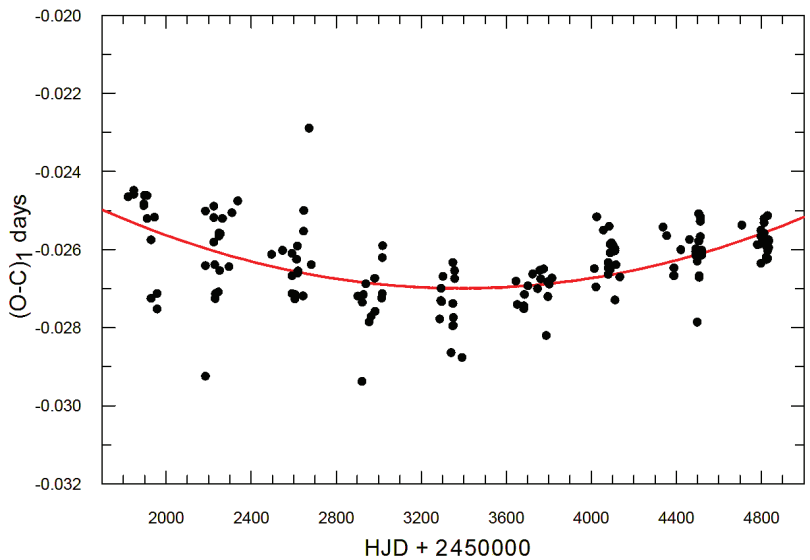

Figure 5. Quadratic least squares fit of residuals (O–C)1 vs HJD for EQ Tau observed between October 5, 2000, and January 4, 2009.

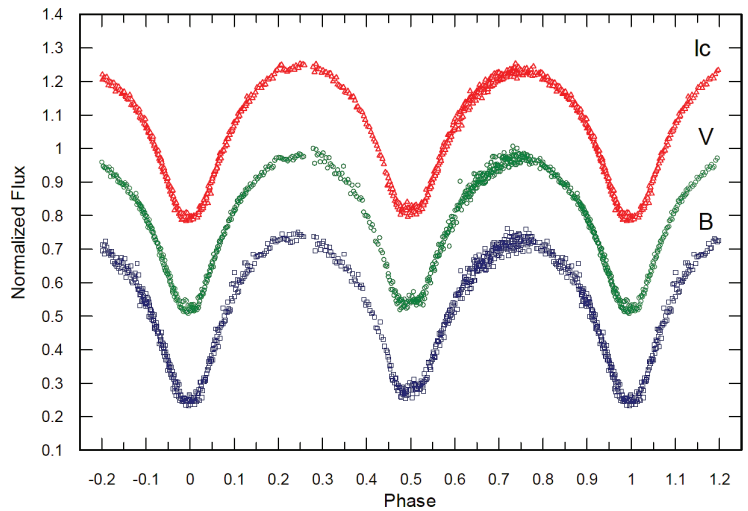

Figure 6. Representative folded CCD-derived light curves for EQ Tau captured in *B*-, *V*-, and *Ic*-passbands (January 26, 2008- March 10, 2008). Light curves are intentionally offset for clarity.

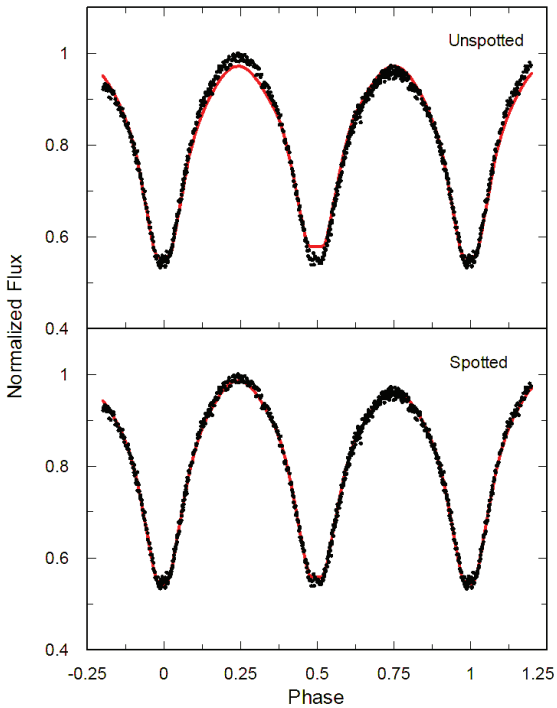

Figure 7. Representative unspotted (top) and spotted (bottom) W-D simulation of light curve for EQ Tau superimposed on CCD observations in *Ic*-passband (2009) from the present study.

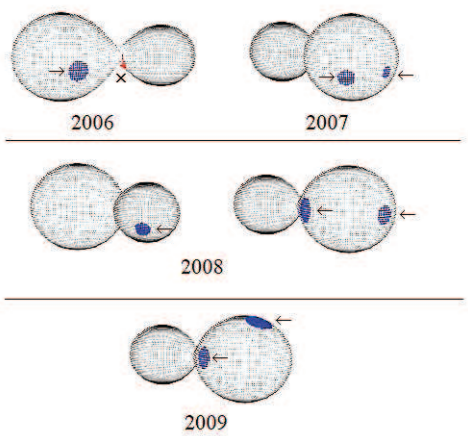

Figure 8. BNINARYMAKER-generated geometric renderings of EQ Tau showing the putative location of starspots from 2006 to 2009. Cold spots are depicted by the arrows while the only hot spot (2006) is marked by the ×.

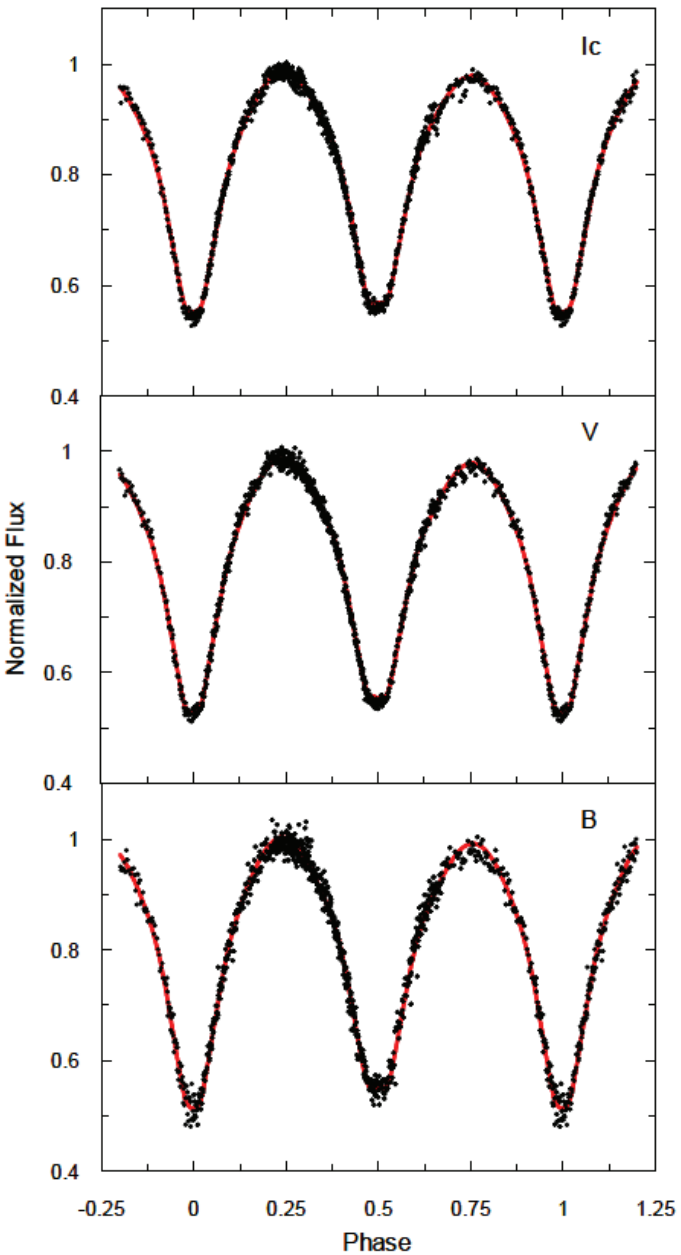

Figure 9. Spotted W-D simulation of 2007 light curves for EQ Tau superimposed on CCD observations in *Ic*- (top), *V*- (middle), and *B*-passbands (bottom) from the present study.

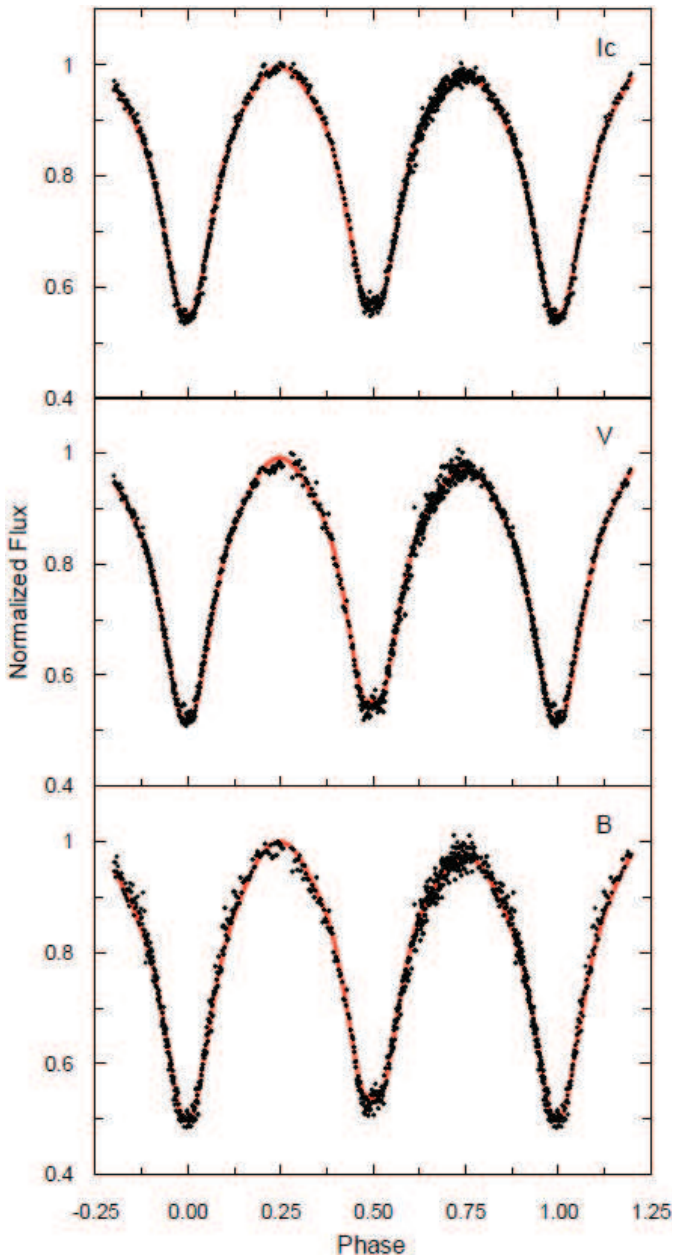

Figure 10. Spotted W-D simulation of 2008 light curves for EQ Tau superimposed on CCD observations in *Ic*- (top), *V*- (middle), and *B*-passbands (bottom) from the present study.

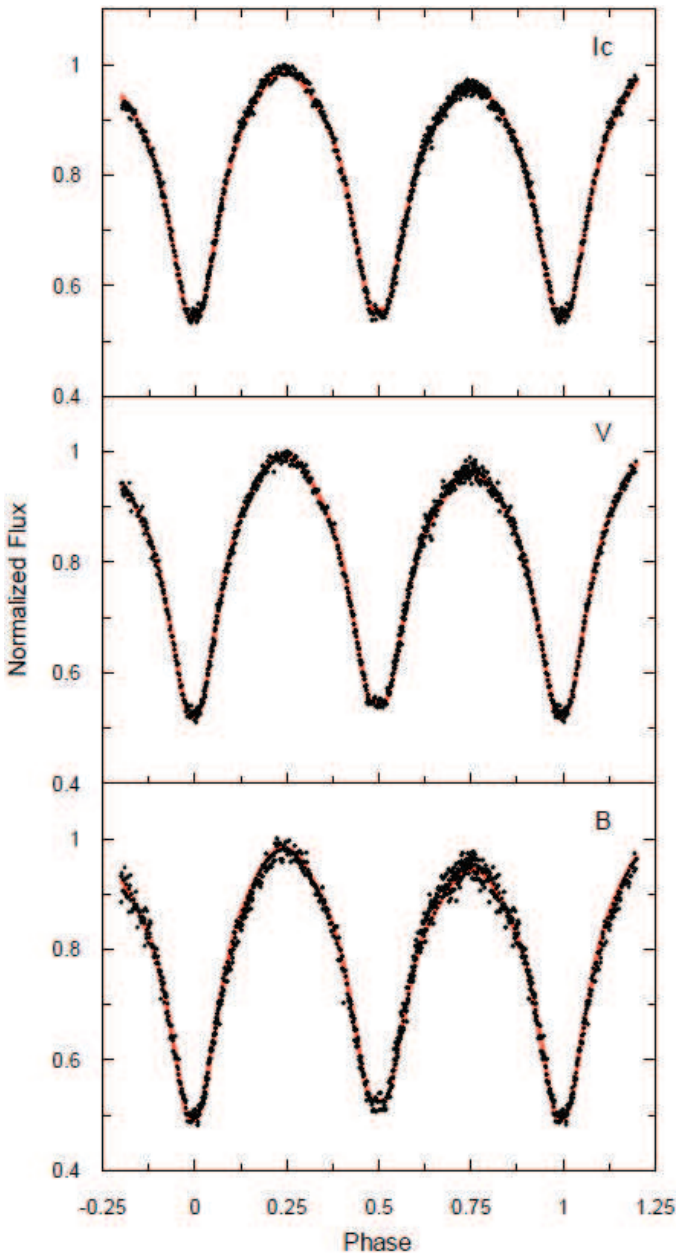

Figure 11. Spotted W-D simulation of 2009 light curves for EQ Tau superimposed on CCD observations in *Ic*- (top), *V*- (middle), and *B*-passbands (bottom) from the present study.

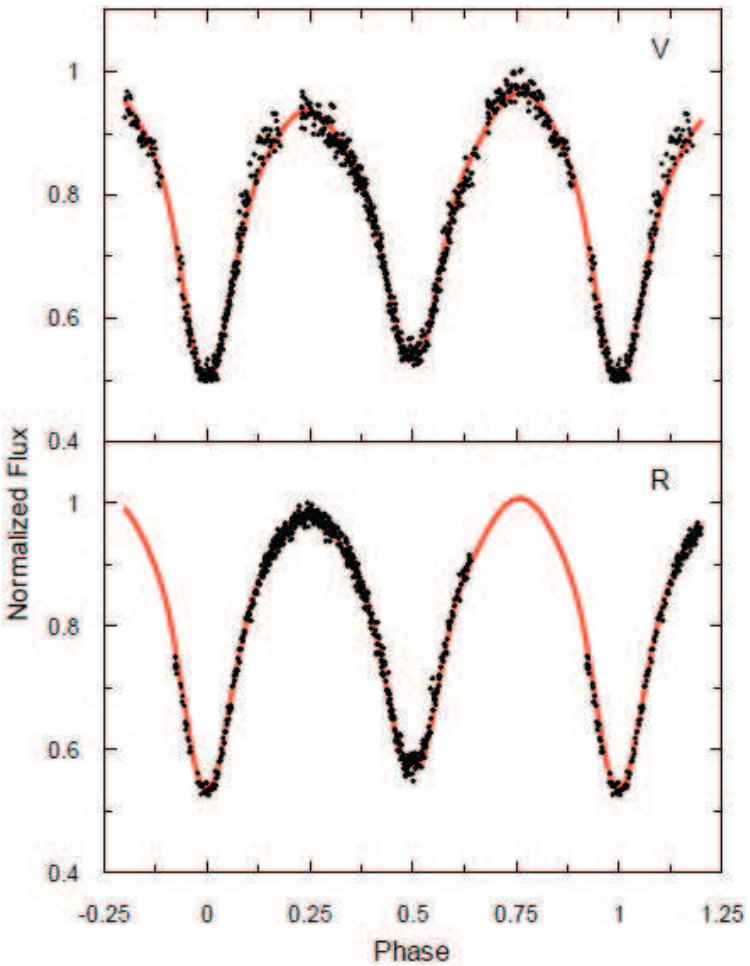

Figure 12. Revised spotted W-D simulation of 2006 light curves for EQ Tau superimposed on CCD observations in *V*- (top) and *R*-passband (bottom) from the present study.